IJCRT.ORG ISSN : 2320-2882

INTERNATIONAL JOURNAL OF CREATIVE RESEARCH THOUGHTS (IJCRT)

An International Open Access, Peer-reviewed, Refereed Journal

Growth and Characterization of semi-organic Potassium Sulfanilate Sesquihydrate (KSSH) single crystals

G. Samuthra[1], N. Prabavathi[1]

[1]Department of Physics, Sri Sarada College for Women (Autonomous), Salem-636016, Tamilnadu, India

Abstract

Potassium Sulfanilate Sesquihydrate (KSSH), semi-organic single crystals were grown by slow evaporation growth technique using water as solvent. The grown crystal subjected to various characterizations. Single crystal X-Ray diffraction study revealed that the KSSH crystal belongs to orthorhombic system. The FTIR study was performed to identify the functional groups present in the grown crystal. Lower cut off wavelength and optical transmission of the grown crystal were found by UV-Visible analysis. The dielectric nature of the crystal was carried out by the dielectric analysis. The mechanical stability and work hardening co-efficient of the KSSH crystal were obtained by Vickers micro hardness measurement. The thermal stability of the compound melting behaviour were carried out TG/DTA analyses. Optical qualities of KSSH crystal were carried out by photoluminescence study.

Keywords: Solution growth; Optical analysis; Dielectrics; Hardness;

1. Introduction

In recent years, there has been considerable interest on the synthesis of semi-organic nonlinear optical materials with excellent nonlinear optical and fluorescence properties, because of their potential applications such as, telecommunication, optical computing, optical data storage, light emitting diodes, and optical information processing [1,2]. A combination of inorganic and organic materials provides a potentially useful approach to more efficient and stable NLO crystals. Metal complexes satisfy very different demands of second order NLO materials such as switchable, tuneable and multidimensional properties depending on the subtle interplay of structure property relationships. It offers a wide range of metals with different oxidation states and ligands, which can be give rise to tuneable electronic properties. Nonlinear optical material (NLO) exhibiting second harmonic generation have been in great demand over the last few decades due to technological importance in the fields of optical communication, signal processing and instrumentation [3]. Semi organic materials gain importance over inorganic materials because of their

large polarizability, wide transmission, and high laser damage threshold [4]. In this view, semi-organic material, Potassium Sulfanilate Sesquihydrate (KSSH) was synthesized and crystal was grown and it yields the nonlinearity of a purely organic ion combined with the favourable mechanical and thermal properties of an inorganic ion. In this present investigation, we report the synthesis, structure, crystal growth and characterization of semi organic material Potassium Sulfanilate Sesquihydrate (KSSH) for the first time in the literature.

2. Experimental procedure

Potassium Sulfanilate Sesquihydrate was synthesized using sulfanilic acid and potassium hydroxide taken in equimolar ration1:1with double distilled water as solvent. The reactants were thoroughly dissolved in double distilled water and stirred well for an hour to yield a homogeneous mixture of solution. The solubility test was carried out with various solvent and found that water is the best. The prepared homogeneous saturated solution was filtered through Whatman filter paper to remove the impurities. Then the clear saturated solution was kept undisturbed in a dust free atmosphere. Crystallization was allowed to take place by slow evaporation technique at room temperature. After the period of 15 days the single crystal with the dimensions 35x30x30 mm^3 was harvested. Grown KSSH single crystal is shown in Figure.1.

Figure.1. Grown KSSH single crystal

2.1 Characterization techniques

The conventional method grown KSSH crystal were subjected to various characterization techniques. The Bruker AXS kappa APEX II diffractometer equipped with monochromatic MoKα radiation (λ=0.710Å) was used to determine the cell parameter and space group of the grown KSSH crystal. The FTIR Spectrum of the grown crystal were recorded in the frequency 400 to 4000cm^{-1} using the KBr pellet technique with Bruker IFS 66/s model at resolution of 40cm^{-1} and with a scanning speed of 2mm/sec. The UV-Visible NIR transmission study were used to

determine the optical property of the grown crystal at the wavelength range of 200-1200 nm using Perkin-Elmer lambda – 35 spectrometer. The photoluminescence (PL) spectrum was recorded by Shimadzu Spectrofluorophotometer LS 4353 model with Xenon arc lamp as the excitation source. The Vicker's microhardness measurement, which is used to determine the mechanical strength of the grown crystal using Shimadzu hardness tester along the 110 plane of the crystal. The dielectric permittivity and dielectric loss of the grown crystal were measured as a function of frequency in the range from 100Hz to 1MHz using model PSM 1735 LCR meter at room temperature. The thermal analysis was carried out in the temperature range of 30ºC - 930ºC using NETZSCH STA 449F3Aanalyzer in nitrogen atmosphere at heating rate of 10ºC/min.

3. Results and discussions

3.1 Single crystal X-ray diffraction (SXRD) analysis

The grown KSSH crystal was subjected to single crystal X-Ray diffraction with a specimen of dimension 0.35x0.25x0.2 mm^3, which was carefully cut from the grown crystal and is mounted on a fibre tube. The data were collected using a Bruker AXS kappa APEX II single crystal diffractometer equipped with graphite monochromated MoKα radiation (λ=0.710Å) at room temperature. The cell parameters were determined from the reflection of 36 frames, measured in three different crystallographic zones. The APEX2, SAINT – PLUS and SADABS programs are used for the data collection, data reduction and absorption corrections performance [5]. A total of 20578 reflection were recorded with 2θ range of 2.77º to 28.32º of which 2298 reflections are considered as unique reflection with I>2σ(I). The structure was solved by direct method procedure and the non-hydrogen atoms were subjected to anisotropic refinement by full-matrix least squares on F^2 using SHELXL-97 program. The position of all oxygen atoms was identified from difference electron density map, and they were constrained to ride on the corresponding K and S atoms. The oxygen atom bound to potassium atoms was constrained to a distance of K-O=2.70-3.18 and bound to S atoms was constrained to a distance of S-O=1.45 with U_{ISO} (K)=3.2 Ueq and (O)=3.6 Ueq [6]. The final refinement converges to R values of R_1=0.0362 and wR_2=0.981. The ORTEP drawing was performed with the ORTEP 3 program [7]. The crystallographic data and the structure refinement parameters of KSSH are presented in Table.1.

Empirical formula	C12 H16 K2 N2 O9 S2
Formula weight	474.59
Temperature	296 (2) K
Wavelength	0.71073 A
Crystal system, space group	Orthorhombic, Pb_{cn}
Unit cell dimensions	a = 22.9979 (15) A°, α = 90 deg. b = 7.704 (5) A°, β =90 deg. c = 10.4254 (8) A°, γ= 90 deg.
Volume	1860.7(2) A^3
Z, calculated density	4, 1.694 Mg/m^3
Absorption coefficient	0.783 mm^{-1}
F(000)	976
Crystal size	0.35 x 0.30 x 0.30 mm
Theta range for data collection	θ_{min}=2.77 θ_{max}=28.32 deg
Limiting indices	h= -30→ 29, k= -10 → 10, l=-1→13
Reflections collected/	20578/2298 [R(int) = 0.0274]
Absorption correction	Semi-empirical from equivalents
Max. and min. transmission	0 .799 and 0.7711
Refinement method	Full-matrix least-squares on F2
Goodness-of-fit on	1.216
Final R indices [I >2sigma (I)]	R1 = 0.0362, wR2 = 0.0981
R indices (all data)	R1 = 0.0380, wR2 = 0.0992

Table -1. Crystal data and structure refinement of KSSH crystal

In the structure, the potassium atom is coordinated by five oxygen atoms. In potassium sulfanilate acid, the potassium adopts distorted pentahedral cubic coordination. The oxygen atom coordinated to K^+ atom are at position x, y, z. The oxygen atoms O1(x,-y,z-1/2), O2(-x+1,-y,-z+1), O3(-x+1,y,-z+3/2), O4(-x+1,-y-1,-z+1) and O5(x,-y,z+1/2) constitute the fivefold coordination of the cubic coordination geometry. The resultant product KSSH contains the sulfanilate anion and potassium cation resulted from the proton transfer. The potassium is linked through the organic backbone of the sulfanilate and the rings to form a three-dimensional structure. The observed lattice parameters values are a= 22.9979 (15) A°, b = 7.704 (5) A°, c = 10.4254 (8) A°, α = β = γ= 90 deg, and volume of the unit cell is 1860.7(2) A^3. The crystal belongs to orthorhombic system with pbcn space group. The K^+ ion forms structural features as consequence of the large radius, adoption of different coordination numbers and the possible occurrence of a stereo-chemically active lone pair. Figure.2. illustrates the molecular structure of KSSH. The unit cell projection along b-axis of KSSH is shown in Figure.3. The observed hydrogen bonds of KSSH are summarized in Table.2. CCDC 1559974 contains the supplementary crystallographic data for this paper. These data can be obtained free of charge via http://www.ccdc.cam.ac.uk/data_request/cifor by emailing data_request@ ccdc.cam.ac.uk or by contacting the Cambridge Crystallographic Data Centre, 12 Union Road, CAMBRIDGE CB21EZ, UK; Fax: +44-01223-336033.

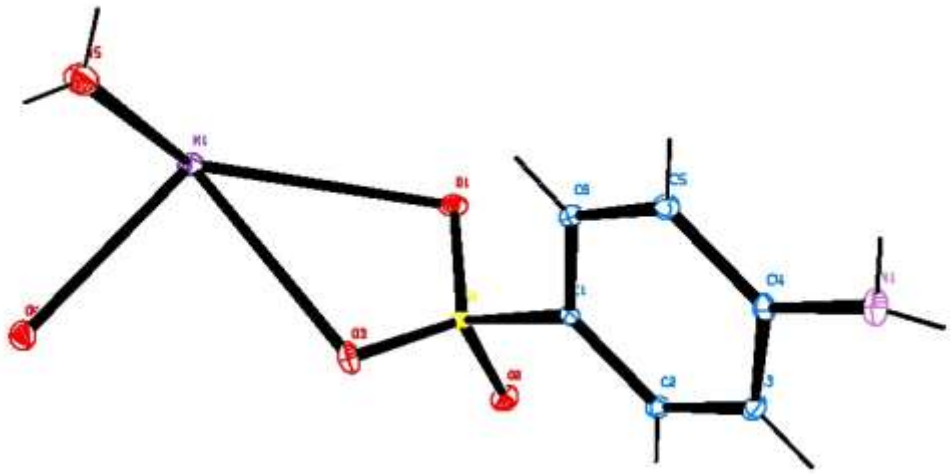

Figure.2 Molecular structure of KSSH crystal

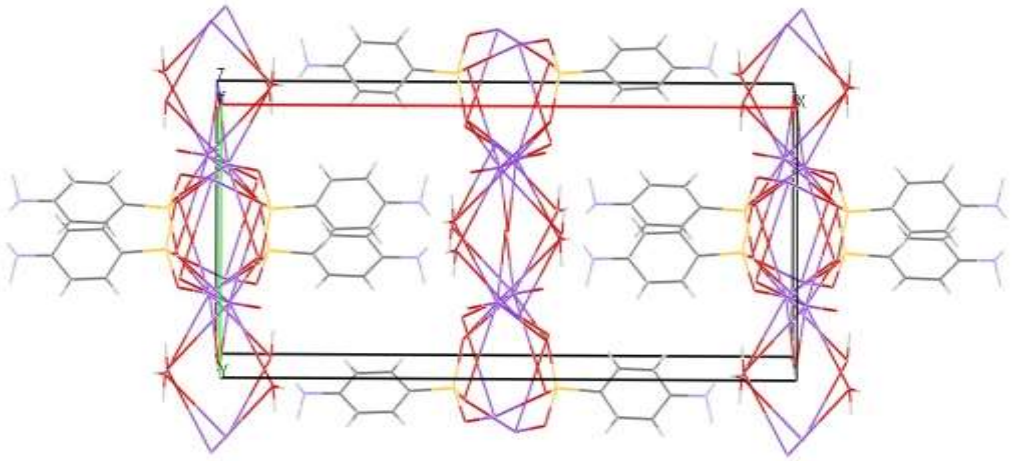

Figure. 3 Packing diagram of KSSH crystal

D-H	d(D-H)	d(H..A)	<DHA	d(D..A)	A symmetry code
N1-H1N1	0.838	2.219	150.49	2.977	O3 [-x+1/2, y+1/2, z]
N1-H2N1	0.847	2.325	179.30	3.172	O5 [-x+1/2, y+1/2, z]
O5-H1O5	0.831	2.081	159.58	2.875	O1 [x, y-1, z]
O5-H1O5	0.831	2.983	156.67	3.761	S1 [x, y-1, z]
O5-H2O5	0.843	2.221	163.22	3.038	N1 [-x+1/2, -y-1/2, z-1/2]

Table -2. Hydrogen bond geometry (Aº) of KSSH crystal

3.2 FTIR analysis

The FTIR Spectra of the grown crystal were recorded in the KBr pellet technique, in the frequency range of 400-4000 cm^{-1} (Bruker IFS 66/s model) at a resolution of 40cm^{-1} and with a scanning speed of 2mm/s shown in Figure.4. The band due to the SO_2 asymmetric stretching vibration of Sulfanilic acid salts occurs at 1250 – 1140 cm^{-1}. The position of the band being mainly dependent on the nature of the metal ion, not on whether the compound is alkyl or aryl. The band is usually broad with shoulders. If the coordination to a metal atom occurs through the Oxygen atom, the S-O stretching frequency decreases when compared with that of the free ligand. In the present study for KSSH the frequency is found to be decreased and the bands observed at 1179 cm^{-1} and 1199 $cm^{-1}$are assigned to SO_2 asymmetric stretching vibrations. The band due to the symmetric stretching vibration is sharper, also has shoulders and occurs at 1070-1030 cm^{-1}. Therefore the symmetric vibrations are assigned to the peaks observed at1034 cm^{-1}, 1008 cm^{-1}. Particularly for Oxygen bonded complexes the band in the region 1025-985cm^{-1} is found to be metal sensitive. The characteristic ranges of wagging and twisting vibrations are 570-450 $cm^{-1}$and 540-400 cm^{-1}. Hence the peaks arised at 567 cm^{-1} and 508 cm^{-1} may be due to the wagging and twisting vibrations of SO_2. The region 730-660 cm^{-1} probably due to the stretching vibration of C-S band [8], which is appeared in IR spectrum at 704 cm^{-1}. In view of literature data, the peak at 3475 cm^{-1} and the other at 3361 cm^{-1} are assigned to the asymmetric and symmetric vibrations of NHα group. The ring C-H vibrations are identified in its characteristic region at 3230 cm^{-1} and 3070 cm^{-1}. The assignments of various functional groups are presented in the Table.3.

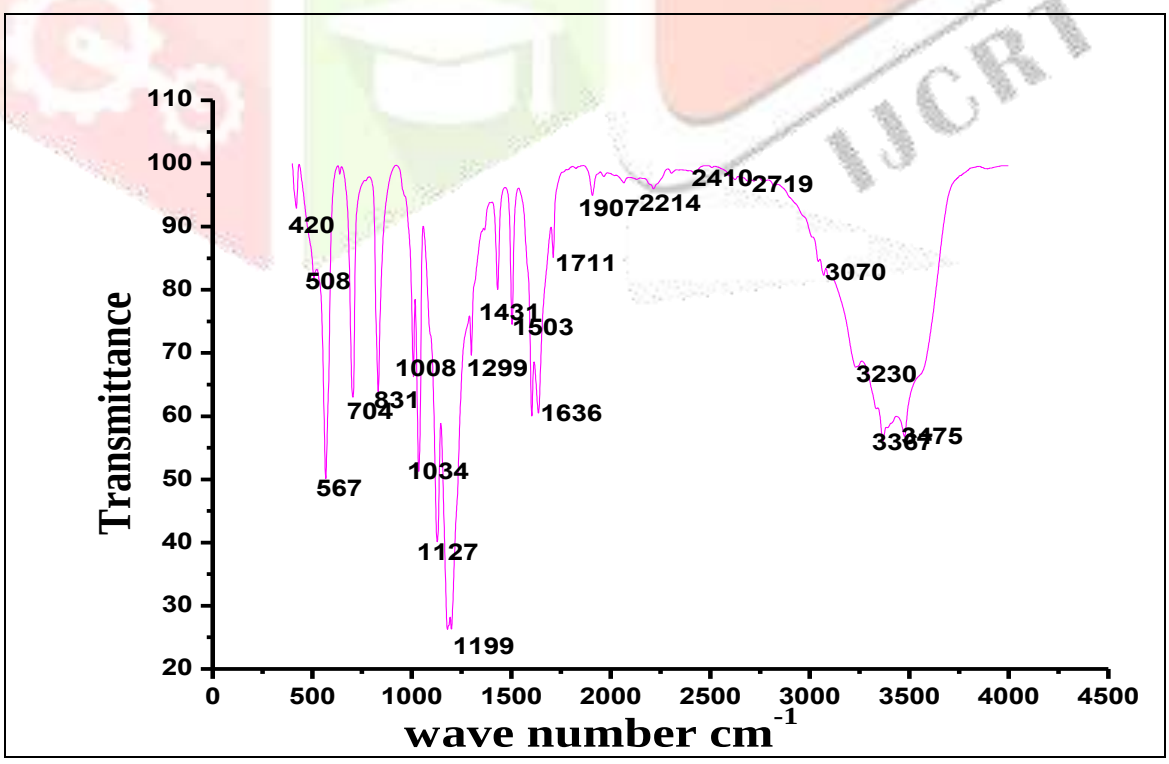

Figure. 4 FTIR Spectrum of KSSH crystal

Wave number cm^{-1}	Assignments
3475, 3361	OH, NH vibrations
3230,3070	C-H stretching
1636	NH_2 Sis
1431	CN Stretching
1199,1179	SO_3 Asymmetric stretching
1127	NH_2
1034,1008	SO_2 Symmetric stretching
704	S-S stretching
567	SO_2Wagging
508	SO_2Twisting

Table - 3 The observed frequencies and corresponding assignments of KSSH crystal

3.3 UV-Visible NIR analysis

The optical property of a material or provide the information about the electronic band structure, localized optical state and types of optical transitions. The transmittance spectrum of the grown crystal has been recorded using Perkin Elmer Lambda-35 spectrometer in the wavelength range 200 – 1200nm covering entire near ultraviolet, visible and high energy part of near IR region. The UV-Visible transmission and absorption spectrum of KSSH was shown in figures 5 and 6.

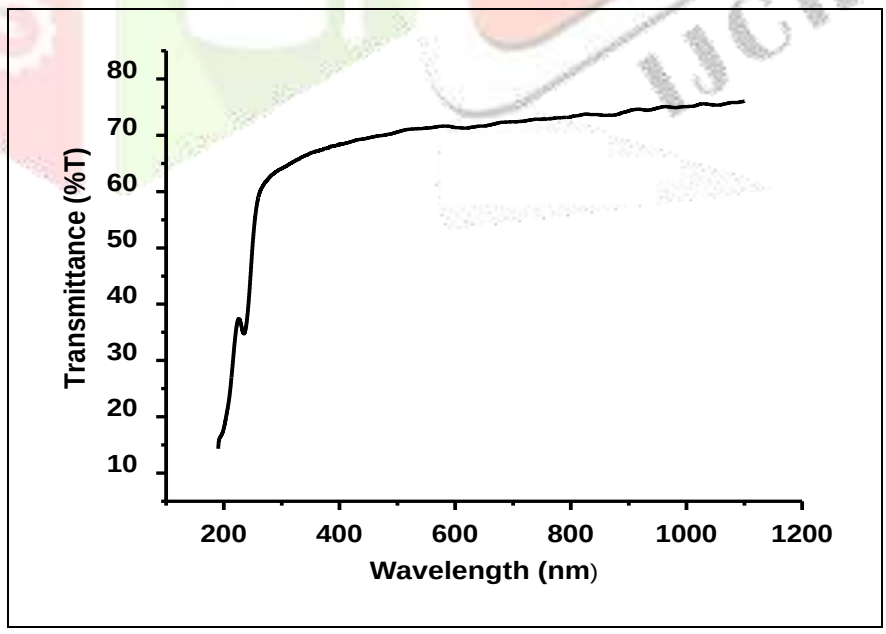

Figure.5 UV-Visible NIR transmittance spectrum of KSSH crystal

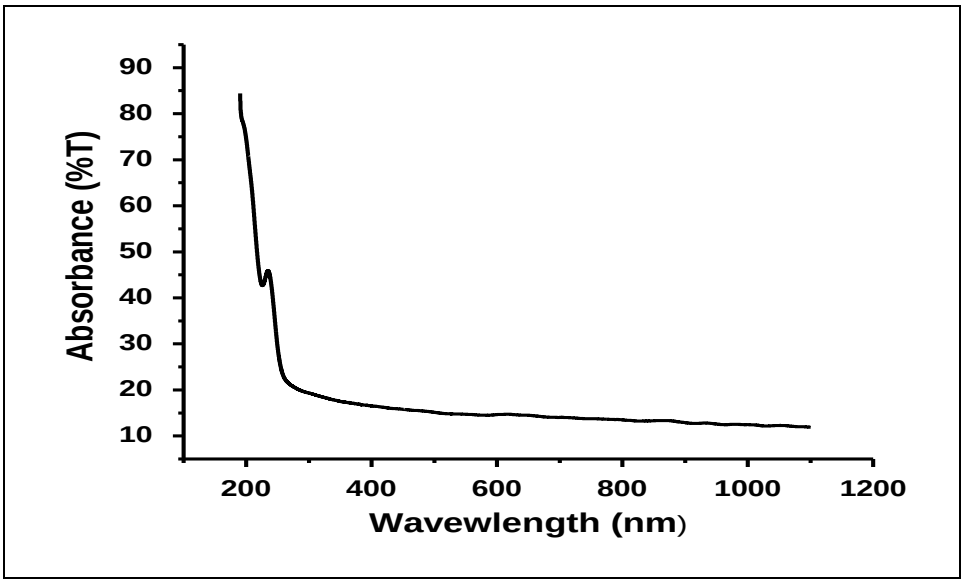

Figure.6 UV-Visible NIR absorption spectrum of KSSH crystal

The lower cutoff wavelength of the grown crystal occurs at 234nm. The recorded UV-Vis-NIR spectrum shows that the grown crystal has good transparency of about 65% in the entire visible and NIR region. The wide transparency of the grown crystal would be much viable for the third harmonic generation for all kinds of laser sources available in the UV-Vis-NIR region. The absorption coefficient (α) is determined using the formula

$$\alpha = \frac{2.3026}{t} \log_{10}\left(\frac{100}{T}\right)$$

Where 'T' is the transmittance (%), 't' is the thickness of the sample (2 mm). The band gap of the KSSH crystal was calculated by Tauc's plot method using the following relation [9].

$$(\alpha h\nu) = A\left(h\nu - E_g\right)^{\frac{1}{2}}$$

Where 'Eg' denotes the optical band gap of the sample, 'A' is a constant 'h' is the Plank constant, 'ν' is frequency of the incident photons and 'n' is the index that characterizes the optical absorption process. The optical band gap of the KSSH was obtained from the UV-Vis transmittance data by plotting graph between energy (hν) and $(\alpha h\nu)^{1/2}$ is shown in Figure.7.

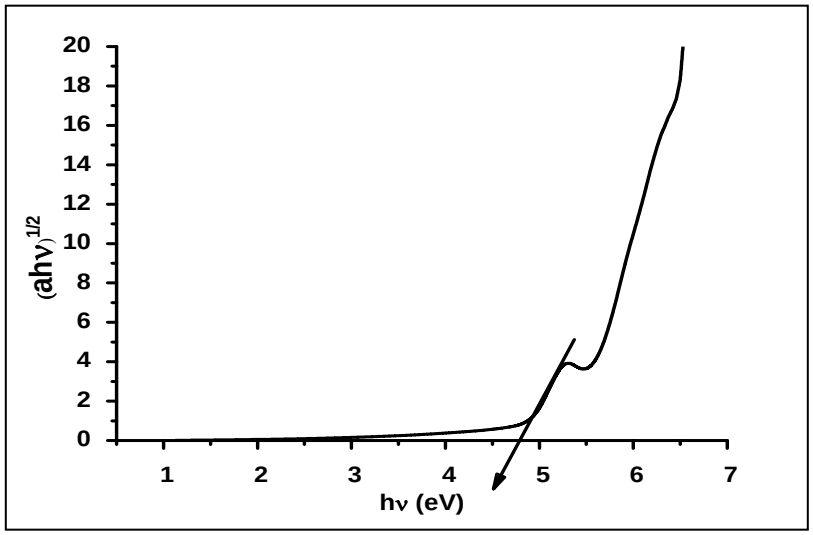

Figure.7 Band gap energy (E_g) of KSSH crystal

The optical band gap energy (E_g) for the conventional grown crystal was calculated by extrapolating the linear portion of the curve to zero absorption and it was found to be 4.7eV. The bandgap energy (5.2eV) of the KSSH crystal was theoretically estimated using the following formula

$$E_g = \frac{hc}{\lambda_{max}}$$

Where h is the Planks constant, c is the velocity of light and λ is the cut-off wavelength (234nm). The obtained band gap is in good agreement with the experimental value. The high band gap value indicates that the grown crystal possess dielectric behavior to induce polarization when influential radiation is incident on the material [10]. In high photon energy region the energy dependence of absorption co-efficient suggests the type of band gap [11]. The transmittance spectrum clearly shows that the crystal having very less defect concentration, which is favourable for linear optical windows and NLO devices.

3.4 Photoluminescence (PL) measurement

The Photoluminescence intensity highly dependent on the crystallinity and structural perfection of the crystal. Fluorescence is generally occurs in molecules that are aromatic which contain multiple conjugated double bonds with a high degree of resonance stability [12]. The photoluminescence spectrum of the crystal was recorded between 260nm-800nm. An intense sharp emission peak occurs at 338nm, owing to the emission of violet radiation and confirms the suitability of the grown material for near violet fluorescence emission. The strong PL emission of the title material may find potential applications in optoelectronic devices [13]. The emission spectra of KSSH crystal is shown in Figure.8.

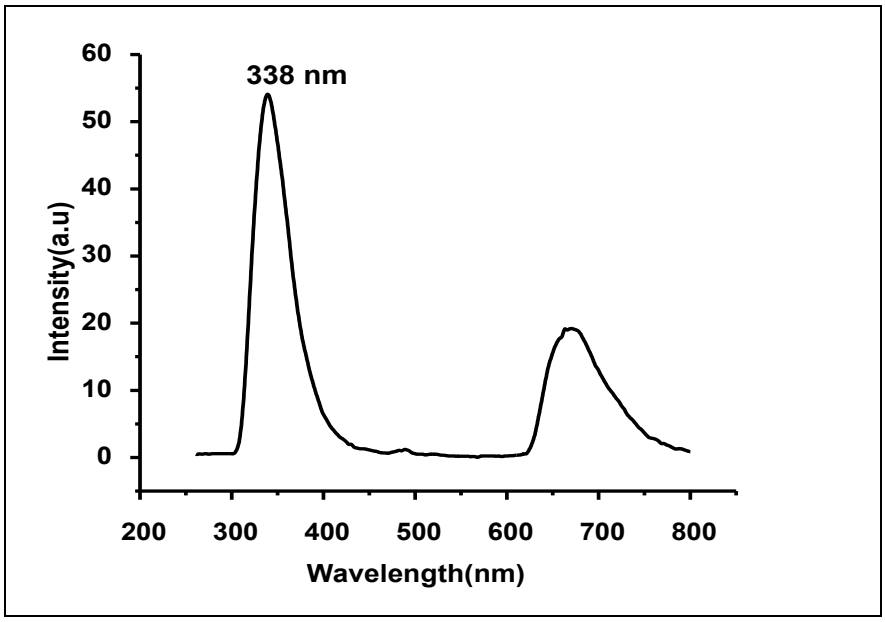

Figure.8 Photoluminescence spectrum for KSSH crystal

3.5 Vickers microhardness test

Vicker's Micro hardness test of the grown crystal was carried out using SHIMADZU micro hardness tester with Vicker's pyramidal indenter, to find out the mechanical strength. The hardness was measured between the load ranges from 25 to 300g. The indentation time was kept constant as 5sec. Each time the average diagonal length was calculated. The relation,

$$Hv=1.8544\ p/d^2 kg/mm^2$$

is used to calculate the hardness number of the grown crystal. Where, **P** is applied load in kg and **d** is the diagonal length of the indentation impression in micrometer and 1.8544 is the constant of geometrical fraction for the diamond pyramid. The Figure.9, clearly indicate that hardness of the grown crystal is increases with increase in load up to 300g (Hv=80.5 kg/mm^2), which indicate that greater stress is required to form dislocation, and thus confirming greater crystalline perfection [14]. An increase in the hardness will have significant effect on device fabrication and processing such as ease in polishing and less wastage due to cracking by polishing.

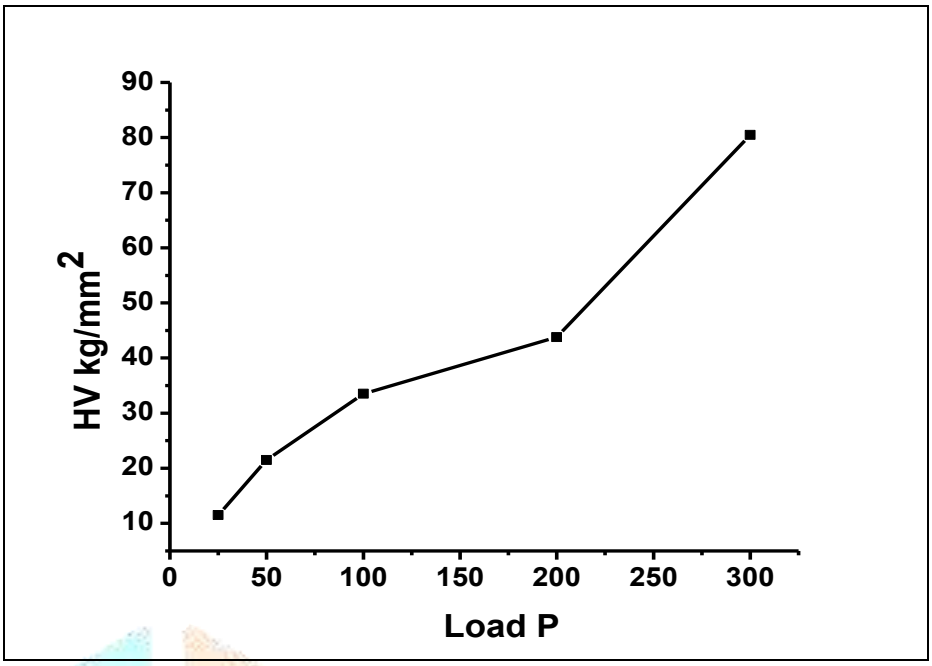

Figure.9 Vickers microhardness plot for grown crystal

The dislocations are generated at the region of the indentation, due to the application of mechanical stress by the indenter. When the applied load is less the indenter point will exert a force on the surface of the crystal is less. While applying higher loads, the indenter will penetrate the surface of the crystal, which is restricted by the movement of dislocations and also the bond strength present in between the neighbouring molecules. The relation between the load P and size of indentation d is given by Mayer's law, $P=Ad^n$ where, **'A'** is a constant and **'n'** is work hardening co-efficient.

By plotting log P verses log d [Figure.10], the value of the work hardening coefficient n was found to be 1.6.According to Onitsch, $1.0 \leq n \leq 1.6$ for hard material and $n>1.6$ for soft material [15]. Hence the grown crystal is a hard material. At the same time low work hardening co-efficient (1.6) indicates that the crystal possesses less dislocations, since work hardening co-efficient is caused by the dislocation present in the crystal.

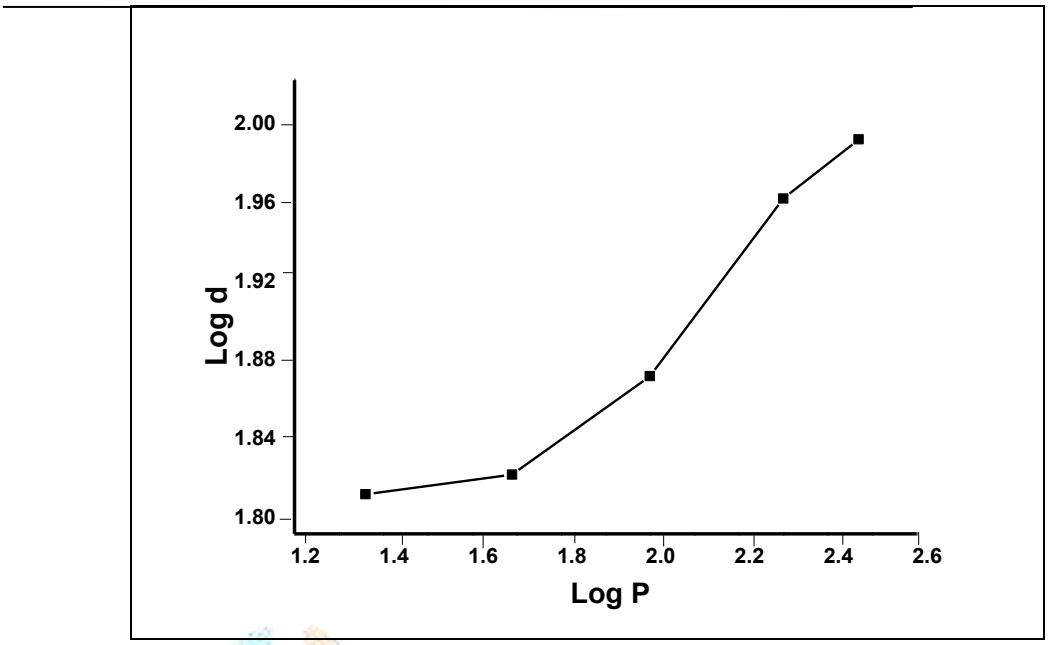

Figure.10 Meyer index graph

3.6 Dielectric measurement

In the current technological society, dielectric based materials have been used extensively in the area of solid state electronics. For the above said applications, the properties that require investigation are the dielectric constant and the dielectric loss factor. The dielectric constant of material is due to the contribution of electronic, ionic, dipolar and space charge polarization, which depend on the frequencies. At low frequencies, all the polarization is active [16]. The dielectric constant and dielectric loss of the grown crystal were measured as a function of frequency in the range 100Hz to 1MHz using numetriq phase sensitive multimeter (PSM 1735) at different temperature. A well-polished transparent and good quality crystal of thickness 2 mm was used and the surface was coated with silver paste in order to make a smooth contact on both sides and make it to behave like a parallel plate capacitor. The frequency dependence of the dielectric constant and dielectric loss of the crystal are shown in Figures.11and12. The variation of dielectric constant with temperature is generally attributed to the crystal expansion, the electronic and ionic polarization and the presence of impurities and crystal defects. The variation of dielectric constant at high temperature is mainly due to the thermally generated charge carriers and impurity dipoles. The decrease of dielectric constant with the increase of temperature is essentially due to the temperature variation of ionic polarizability.

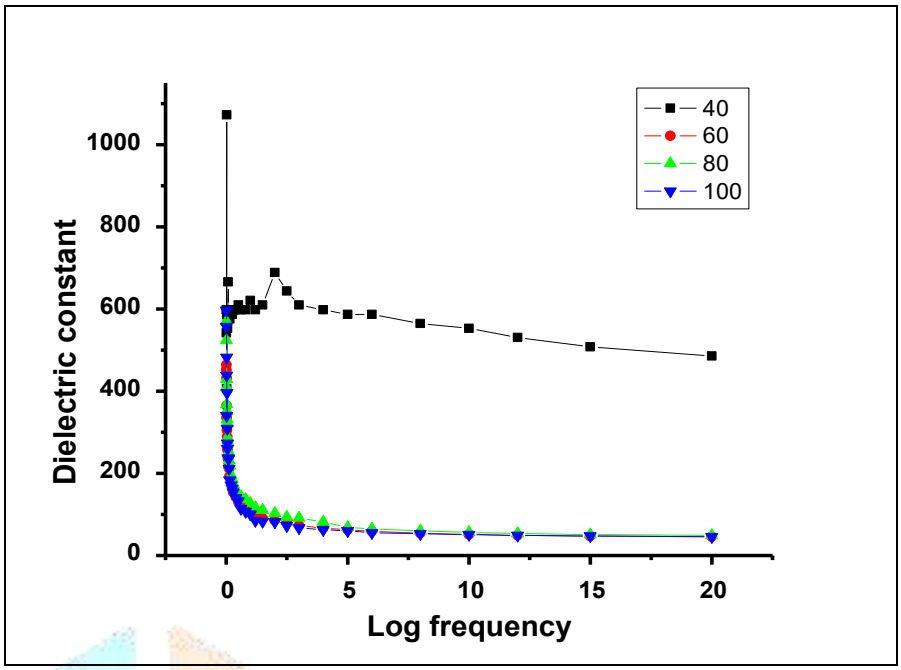

Figure.11 Dielectric constant for grown crystal

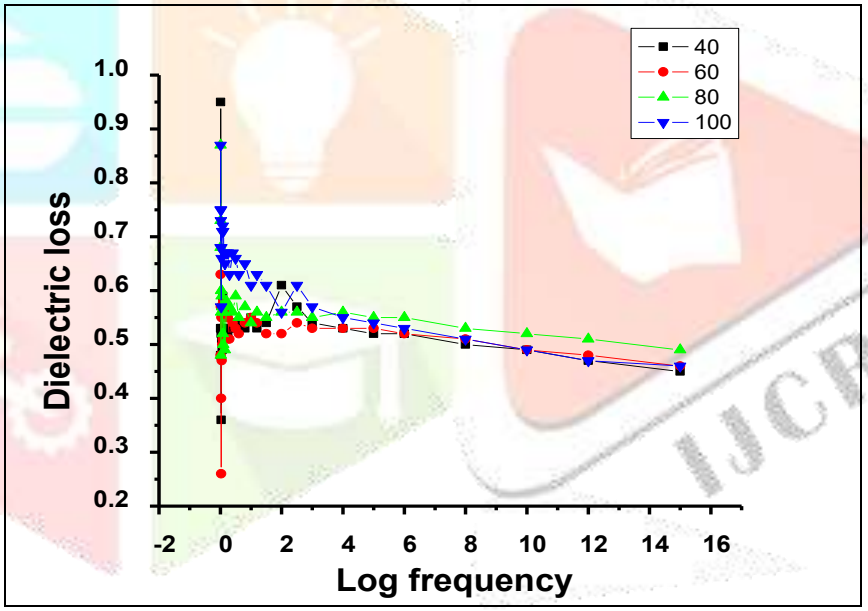

Figure.12 Dielectric loss for grown crystal

Moreover the space charge of the dielectric properties of the NLO materials is closely associated with the refractive index and related optical properties of the material. The relatively high dielectric constant of the material at room temperature is a good indication for NLO effects since high dielectric constant induces large poles, when the material is exposed to high intense electromagnetic radiation such as laser. In accordance with Miller rule [17] the lower value of dielectric constant at higher frequencies in a suitable parameter for the enhancement of SHG co-efficient. The dielectric loss curve clearly indicates that the dielectric loss increases with increase of temperature and decreases with increasing the frequency, which indicates that the crystal is almost free from structural defects. This

parameter plays a crucial role for the construction at devices for non-linear optical materials (Balarew&Dushlew 1994).

3.7 Determination of solid state parameters (SSP)

Solid state parameters are important in electro-optic polarizability of the material and it is essential for the desired efficiency of nonlinear effect. Theoretical calculation shows that the high-frequency dielectric constant explicitly depends on the valence electron Plasma energy, Penn gap, Fermi energy and electronic polarizability of the material. The density of KSSH single crystal is calculated by the following equation

$$\rho = \frac{MZ}{N_A V} \tag{1}$$

Where 'M' is the molecular weight of the grown crystal in g/mol, 'Z' is a molecular unit cell, 'N_A' is Avogadro's number (6.023×10^{23}) and 'V' is the volume of the unit cell in $Å^3$. The valence electron plasma energy ($\hbar\omega_P$) is given by [18]

$$\hbar\omega_p = 28.8\left(\frac{Z'\times\rho}{M}\right)^{\frac{1}{2}} \tag{2}$$

Where 'M' is the molecular weight and 'ρ' is the density of KSSH crystal. The total number of valence electrons (Z') of KSSH crystal is 142 and it has been calculated from the following formula

$$Z' = [(12\times Z'_C) + (16\times Z'_H) + (2\times Z'_N) + (2\times Z's) + (2\times Z'K)]) + (9\times Z'_O)] \tag{3}$$

According to the Penn model [19], the average Penn gap (E_P) and Fermi energy (E_F) [20] of KSSH crystal are calculated using the following relations

$$E_P = \frac{\hbar\omega_p}{(\varepsilon'-1)^{\frac{1}{2}}} \tag{4}$$

$$E_F = 0.2948\ (\hbar\omega_p)^{\frac{1}{2}} \tag{5}$$

Where 'ε'' is the dielectric constant of the conventional method grown crystal at 1 MHz. The value of electronic polarizability (α) is calculated from the KSSH crystal using the following relation (6)

$$\alpha = \left[\frac{(\hbar\omega_p)^2 S_0}{(\hbar\omega_p)^2 S_0 + 3E_p^2}\right]\times\frac{M}{\rho}\times 0.396\times10^{-24}\,cm^3 \tag{6}$$

where, 'S_0' is a constant for a particular material which is given by

$$S_0 = 1 - \left[\frac{E_p}{4E_F}\right] + \frac{1}{3}\left[\frac{E_p}{4E_F}\right]^2 \quad (7)$$

The value of electronic polarizability (α) of the conventional method grown KSSH crystal was calculated using the following Classius-Mossati relation (8)

$$\alpha = \frac{3M}{4\pi N_A \rho}\left(\frac{\varepsilon' - 1}{\varepsilon' + 2}\right) \quad (8)$$

The value of electronic polarizability (α) also can be obtained using the optical band gap, which is given as

$$\alpha = \left[1 - \frac{\sqrt{E_g}}{4.06}\right] \times \frac{M}{\rho} \times 0.396 \times 10^{-24} cm^3 \quad (9)$$

Where 'E_g' is the optical band gap energy (4.7eV).All these calculated parameters for the KSSH crystal are listed in Table.4. It reveals that the calculated electronic polarizability of the conventional method grown KSSH crystal is higher than standard KDP crystal.

Parameters	KSSH crystal
Plasma energy $\hbar\omega_p$ (eV)	20.50
Penn gap energy E_P (eV)	4.87
Fermi energy E_F (eV)	16.54
Electronic polarizability (α) using Penn analysis (cm^3)	9.37×10^{-23}
Electronic polarizability (α) using Clausius-Mossoti equation (cm^3)	9.49×10^{-23}
Electronic polarizability (α) using optical band gap (cm^3)	6.30×10^{-23}

Table -4. Electronic polarazibilty (α) results based on dielectric analysis

3.8 Thermal analysis

The thermal behaviour of the grown crystal was carried out by the TG/DTA analysis. The sample weight of 3.780 mg was taken for the measurement. The thermal analysis of the KSSH crystal was carried out in the temperature range 25ºC to 1400ºC with the heating rate 20ºC/min in nitrogen atmosphere using TGAQ 500 V 20 model TG/DTA instrument, and the resulting thermogram is shown in Figure.13.

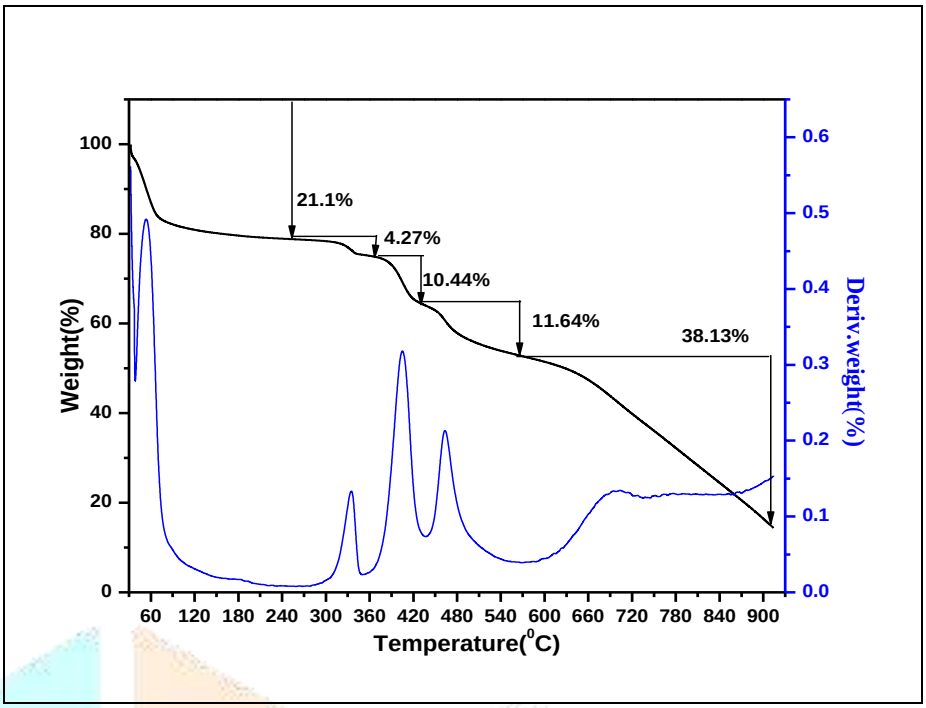

Thermo gravimetric and differential thermal analysis gives the information about the phase transition, water of crystallization and different stage of decomposition and melting point of the crystal. The DTA thermogram reveals that the material undergoes an irreversible exothermic transition at 78.6ºC and 402ºC. The weight loss at 78.6ºC and 402ºC is due to liberation of volatile substance like oxide of potassium and hydrogen leading to significant decomposition of the material. The weight loss at the temperatures 253ºC and 375.72ºC relates to release of N_2 and [3(H_2)] respectively and which are exothermic character. The major weight loss is observed between 574ºC and 912ºC. The next major weight loss is occurred in the range 32ºC to 250ºC. All the peak of TGA trace is matching with the intense weight loss in the DTA curves. The sharpness of endothermic peak shows the good degree of crystallinity and purity. The weight loss between the two successive decomposition temperatures is shown in Table.5.

S.No	Temperature range (°C)	Weight loss (%)
1	52.69°C-253.60°C	21.11
2	253.60°C-375°C	4.272
3	375°C-444.41°C	10.44
4	444.41°C-574.16°C	11.64
5	574.16°C-912°C	38.13

Table – 5. The weight loss between the two successive decomposition temperatures for KSSH Crystal

4. Conclusions

The good quality transparent KSSH single crystal was grown successfully by slow evaporation method. From single crystal X- Ray Diffraction analysis the lattice parameters were observed as a = 22.99, b = 7.76, c = 10.42, α = β= γ= 90°. Thus, it crystallizes in orthorhombic system with Centro symmetric space group. The cell parameters, space group of the crystal are determined using X-Ray diffraction analysis. The functional groups are identified using FTIR spectrum. The optical transmission analysis revealed that the crystal has high percentage at transmission in the entire UV-Visible NIR region, which is very essential for the NLO crystals. The wide range of transparency is an added advantage in the field of electronic applications also. PL studies show that the crystal has a violet fluorescence and the emission occurs at 338 nm. Higher mechanical stability indicates greater stress required to form dislocation thus confirming greater crystalline perfection. The less value of work hardening co–efficient (n) also confirms this result. The observed low dielectric loss at higher frequencies suggests that the crystal possesses enhanced optical quality with fewer defects and this parameter is of vital importance for various NLO materials and their application. The thermal stability, melting point, decomposition stages of the grown crystal were analyzed using TGA/ DTA studies.

Acknowledgements

The authors are thankful to SAIF, IIT-Madras for single crystal XRD analysis and TG/DTA. We also thank NCIF, National College, Tiruchirappalli for Vickers microhardness studies, ACIC, St. Joseph's College, Tiruchirappalli for PL measurement, dielectric and FTIR analysis.

References

1. Wiliams J (ed) American Chemical Society Symposium Series 233, American Chemical Society, Washington DC (1983).
2. Chemla DS, Zyss J (eds) Academic press, New York vol 1 and 2, (1987).
3. BhadeshiaH.K.D.H,University of Cambridge, Material Science and Metallurgy.
4. Mohan Kumar R, RajanBabu D, Jayaraman D, Jayavel R, Kitamura K,J Crys Growth 275 (2005) e1935–e1939.
5. Bruker-Nonius AXS APEX2 and SAINT Bruker-Nonius AXS, Madison (2004).
6. Sheldrick GM, ActaCryst A64, (2008) 112–122.
7. Farrugia LJORTEP-3 program for molecular drawing. J ApplCryst 30, (1997) 565–569.
8. G.Socrates, Infrared Characteristic Group Frequencies, wiley New York, 1980.
9. J.Tauc, R.Grigorovici, A.Vancu, Physica Status Solidi, 15, (1966), 627-637.
10. P.Vasudevan, S.Gokul Raj, S.Sankar, Spectrochimica Acta Part A:106, (2013), 210-215.
11. P Singh, A K Chawla, D Kaur, R, Chandra Materials Letters 61(10), 2050-2053 (2007).
12. Skoog, Douglas A, Principles of instrumental analysis. Holt, Rinehart & Winston, New York (1971).
13. Subhadra K G, KishanRao K, Sirdeshmukh D B, Bull Mater Sci, 23, (2000) 147-150.
14. S. Balamurugan, P.Ramasamy, Mater. Chem.Phys. 112(2008)1.
15. E.M Onitsch, Mikroscopia 2(1947) 131.

16. P.A. Varotsos, J. De. Phys. Lett. 39, 1978, L-79.

17. C. Miller, Applied Physics Letter, 5 (1964) 17.

18. J. D. Jackson, Classical Electrodynamics, Wiley Eastern, (1978), 321.

19. D. R. Penn, Physical Review, 128, (1962), 2093–2097.

20. C. Balarew and R. Duhlew, Journal of Solid-State Chemistry, 551(1984), 1–6